Framework for Preventive Control of Power Systems to Defend Against Extreme Events

Yuwei Xiang, Tong Wang, *Member*, *CSEE*, and Zengping Wang, *Member*, *CSEE*

***Abstract*—Enhancing power system resilience against extreme events is becoming increasingly critical. This paper discusses a unified framework for preventive control of power systems to enhance system resilience, which includes three parts: resilience assessment, resilience grading, and resilience enhancement. First, the resilience assessment contains facility-level and system-level resilience assessment. The concept of fragility curve is used in the facility-level resilience assessment. Various resilience indices are developed in system-level resilience assessment to roundly depict the impacts of extreme events on power systems and determine the system resilience. On this basis, the resilience is divided into different levels by resilience grading strategy, which can efficiently quantify the severity of the impact of extreme events and provide decision-making for the resilience enhancement strategies. Then, control strategies for enhancing power system resilience are also divided according to different resilience levels. A controlled islanding based preventive control is proposed to enhance system resilience, which aims to strengthen the first defensive line of power systems to deal with extreme events. Finally, taking the typhoon disaster in extreme events as an example, two tests carried out with two typhoons demonstrate the efficiency of the proposed method.**

***Index Terms*—Controlled islanding, extreme events, power system resilience, preventive control.**

I. Introduction

EXTREME events, such as typhoons and snowstorms, occur frequently, which often causes severe damages and even blackout accidents to power systems. For example, a strong typhoon Rainbow hit the southern power grid of China in 2015, causing more than a thousand lines and over one hundred substations outage, furthermore, the power supply of above 4 million customers was interrupted for several days [1]. In 2021, more than 4 million people in Texas of U.S. are out of power due to an extremely cold weather event. The blackout of Texas further induced a dramatic increase of electricity prices and the interruption of daily necessities such as water and gas, which exerted a significant impact on people's lives [2].

Manuscript received October 25, 2022; revised January 28, 2023; accepted February 27, 2023. Date of online publication June 27, 2023; date of current version July 25, 2023. This work was supported by the Science and Technology Project of State Grid Corporation of China "Cooperative Control and Protection System and Application of Power System with Renewable Energy Sources" (5100-202199530A-0-5-ZN, 5211DS21N013).

Y. W. Xiang, T. Wang (corresponding author, email: hdwangtong@126.com; ORCID: https://orcid.org/0000-0002-1950-9742), and Z. P. Wang are with the State Key Laboratory of Alternate Electrical Power System with Renewable Energy Sources, North China Electric Power University, Beijing 102206, China.

DOI: 10.17775/CSEEJPES.2022.07290

Therefore, it is crucial to ensure the safe operation and reliable power supply for power systems under extreme events. To this end, a concept of "resilience" coming from ecology [3] was proposed to help power systems defend against extreme events. Resilience refers to the ability of power systems to resist to high-impact and low-probability extreme events [4], [5]. In this context, the impacts of extreme events on power systems can be effectively quantified by resilience assessment. Then, corresponding resilience control strategies can contribute power systems to enhance the resilience and resist extreme events. Hence, enhancing power system resilience relies on the resilience assessment, and both are an organic whole in facing extreme events, which deserves to be studied in depth.

A. Literature Review

Much research has been conducted on the resilience assessment and resilience enhancement strategies to resist extreme events [6], [7]. Resilience assessment of power systems can be categorized into facility-level resilience assessment and system-level resilience assessment. The essence of the facility-level resilience assessment is to evaluate the damage probability of power facilities during extreme events. The fragility curve can effectively relate the damage probability of power facilities to the intensity of extreme events. Thus, it has been extensively applied to assess the resilience of power facilities [8], [9]. The system-level resilience assessment is mainly to use related resilience indices to assess the impacts of power facility damage on power system operation. In [10], the expected load loss due to typhoons is defined as the resilience indices to assess system resilience. On the basis of this, the frequency of load loss is defined in [11], [12] to assess system resilience during extreme events. In [13], several resilience metrics were proposed to quantify system resilience, then the amount of generation capacity and load demand that are connected during extreme event are adopted as resilience assessment indices to quantify these resilience metrics.

Following the resilience assessment, resilience control strategies are available to enhance power system resilience when the resilience diminishes. The resilience enhancement strategies mainly consist of physical strategies and operational strategies. Reinforcing power facilities before extreme events is a typical physical strategy to enhance system resilience [14]. In practice, Texas ever planned to improve transmission line design standards to defend against hurricanes [6]. However, the reinforcement strategy suffers high costs and may not be always sufficient to cope with extreme events. Therefore,

much research has focused on using operational strategies to enhance system resilience, where the emergency response and load restoration techniques applying energy storage system (ESS) [15], [16], microgrids (MGs) [17], [18], and distribution energy resources (DERs) [19] have been extensively discussed. The core of these control techniques is to coordinate and configure MGs, ESS, and DERs to ensure power supply during extreme events and then enhance the system resilience. Except for the above post-event control techniques, preventive control executed before extreme events is also a feasible resilience enhancement strategy. In [20], a preventive control strategy considering generator re-dispatch and topology switching was proposed to boost power system resilience. A controlled islanding based preventive control strategy was proposed in [21] to enhance the system resilience.

B. Research Gaps

From above research, current resilience assessment indices are mainly defined from the generator side and load side, and merely reflect the impact of extreme events on power system resilience from the load loss and generator loss. However, the impact caused by extreme events are not just load loss or generator loss. The security and stability of the whole power system are also extremely easy to be influenced by extreme events. Nevertheless, rarely has literature assessed power system resilience from these aspects. Therefore, the resilience assessment indices are well worth further research.

In terms of resilience enhancement strategies, the control methods for enhancing the resilience can be categorized into two types from the above research, i.e., preventive control and post-event control. Much literature has been devoted to the post-event control. For instance, the MGs, ESS, and DERs have been extensively applied to enhance system resilience. Nevertheless, when the impact of extreme events on power systems is very great, the post-event control often fails to effectively improve system resilience, which may not represent desirable control effects. However, because the preventive control is executed before accidents and the accidents have not influenced power systems at this moment, it can often well enhance power system resilience in this case. Moreover, since the preventive control is carried out before the post-event control, it can dramatically reduce the burden of post-event control, which helps the post-event control jointly defend against extreme events. However, the preventive control under extreme events, especially the preventive controlled islanding, has only attracted minimal attention. Only little literature, such as [21], proposed a preventive controlled islanding to boost system resilience. In [21], the vulnerable lines with higher outage probability caused by extreme events were isolated into one island in advance using the preventive controlled islanding. Hence, the impact of extreme events is effectively prevented to be spread to the rest of the network. The rest of the system can operate safely, but the island that is isolated is ignored after [21]. In other words, the method of [21] aims to enhance the resilience of the remaining system by sacrificing an island, which is more suitable for the extreme events with more concentrated influence range. If the influence range is scattered, and vulnerable lines are with far electrical distance due to extreme events, then the isolated island is larger and more loads may be lost. Hence, the preventive controlled islanding deserves to be further studied.

In summary, existing methods have made great contributions in the field of power system resilience, but they may have the following issues which deserve further investigation.

1) Current resilience assessment indices are mainly defined based on load and generator loss, which is relatively single and hard to comprehensively reflect the impact of extreme events on the safe and stable operation of the whole system.

2) Most of resilience enhancement strategies focus on post-event control but less on the preventive control. In other words, the first defensive line of power systems plays a weak role in dealing with extreme events.

3) It is lack of a complete and effective execution framework for preventive control when the preventive control is applied to enhance power system resilience.

C. Contributions

To address the above issues, this paper proposes a unified framework for preventive control of power systems to enhance system resilience against extreme events, which includes resilience assessment, resilience grading, and resilience enhancement. In terms of resilience assessment, the facility-level and system-level resilience assessment are respectively discussed, and various resilience assessment indices are developed from the perspective of safe and stable operation of the whole system. The resilience grading strategy is proposed to quantify the resilience level, and then provides decision-making for the resilience enhancement strategy. The resilience enhancement strategy is categorized as preventive control and post-event control strategy in this paper, where the preventive control is the research focus. A controlled islanding based preventive control is proposed to enhance system resilience. The main contributions of this paper can be summarized as threefold:

1) A framework for preventive control is proposed in this paper to enhance power system resilience under extreme events, which includes three components: resilience assessment, resilience grading, and resilience enhancement.

2) The resilience assessment indices are defined from the security and stability of power systems in this paper, which can comprehensively and effectively reflect the impact of extreme events on the system resilience. Then, a wooden barrel theory based resilience grading strategy is proposed to quantify system resilience level, which can provide effective decision-making for the preventive control.

3) A preventive controlled islanding (PCI) is proposed to enhance power system resilience. The lines vulnerable to extreme events are included in the splitting surface, which will be removed by the PCI before extreme events to eliminate their impacts on the system. The proposed PCI aims to strengthen the role of the first defensive line of power systems to defend against extreme events, and ensure reliable power supply to all loads as much as possible.

D. Organization

The remainder of the paper is organized as follows: Section II provides a conceptual framework of preventive control

under extreme events; In Section III, resilience assessment indices, a resilience grading strategy, and a PCI strategy are discussed; Section IV takes the typhoon disaster in extreme events as an example to verify the proposed method by simulation tests; The conclusions are provided at the end of this paper.

II. The Overall Framework of Preventive Control

The proposed framework of preventive control under extreme events is shown in Fig. 1.

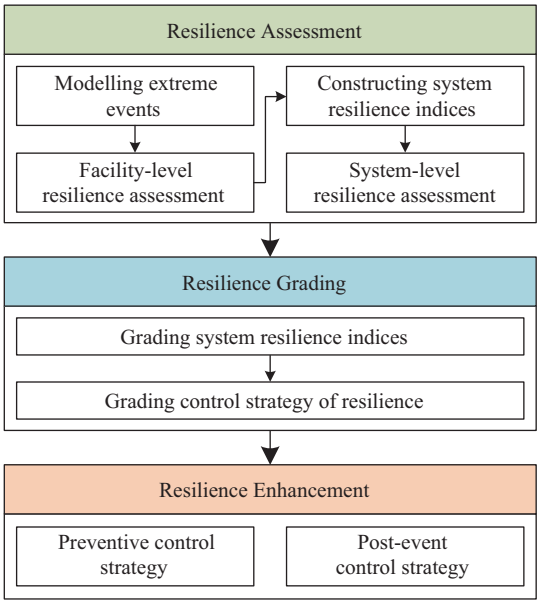

Fig. 1. The conceptual framework of preventive control.

A. Resilience Assessment

The resilience assessment consists of facility-level and system-level resilience assessment. Since power facilities, such as transmission lines and towers, are the first to be damaged by extreme events, the resilience assessment of power facilities needs to be first conducted. The damage probabilities of power facilities can be obtained using the prediction information of extreme events and their models. Then, the outage probabilities of all lines caused by the damage of facilities can be determined, and the lines holding outage probability higher than a specified probability threshold are viewed as vulnerable lines, which are used to form the contingency set before extreme events.

The system-level resilience assessment aims to use various reasonable resilience assessment indices to quantify the system resilience after these vulnerable lines tripped. Hence, the resilience assessment indices are crucial in this case. Two important factors, comprehensive and effectiveness, are considered in this paper to construct these indices. To this end, various resilience assessment indices consisting of the security and stability of the whole system are adopted in this paper to comprehensively and effectively assess the system resilience.

B. Resilience Grading

The power system resilience under extreme events can be fairly assessed based on the first component "resilience assessment". However, the severity of the impact of extreme events on power systems, i.e., the system resilience level, is hard to be determined only by the resilience assessment results. Furthermore, it is hard to decide if the control strategies for enhancing the system resilience need to be executed and which control strategies need to be carried out.

To address the above concerns, a resilience grading strategy is proposed in this paper. The resilience grading is a bridge that can coordinate the resilience assessment and resilience enhancement. Each resilience indicator will be graded into three levels according to its severity in this paper. Then, a well-known barrel theory is applied to grade the resilience of the whole system, which provides effective decision-making for resilience enhancement strategies. Moreover, the resilience enhancement strategies are also graded. Aiming at different resilience levels, detailed control guidelines and control methods are formulated in this paper to enhance the resilience.

C. Resilience Enhancement

The final component of the framework is "resilience enhancement". In this paper, the control strategies for enhancing system resilience are divided into two types, the preventive control strategy and the post-event control strategy. The preventive control is available at the first defensive line of power systems [22], but it plays a weak role in resisting extreme events. To this end, a PCI is proposed to strengthen the role of preventive control of the first defensive line to defend against extreme events. Controlled islanding, also called as system splitting, has been extensively used as the last resort of power system stability control [23]–[26], and it is usually executed after accidents. This paper is devoted to bringing the controlled islanding forward to the first defensive line, and expands the performance of controlled islanding to enhance the power system resilience against extreme events.

III. Resilience Assessment and Enhancement Methods

In the Section II, an overall framework for preventive control of power systems is developed. This section will detail each component of the framework.

A. Constructing Resilience Assessment Indices

The generic fragility curve shown in Fig. 2 relates the outage probability of power facilities to the extreme event intensity, which has been extensively applied to facility-level resilience assessment [8]–[15]. Thus, facility-level resilience assessment is not the focus of this paper, and the fragility curve obtained by [8] is used to assess the facility-level resilience.

The system-level resilience assessment needs to be conducted after the facility-level resilience assessment. To construct effective and comprehensive resilience assessment indices, two concerns have drawn the attention of this paper. The first concern is that the resilience assessment is not involved in

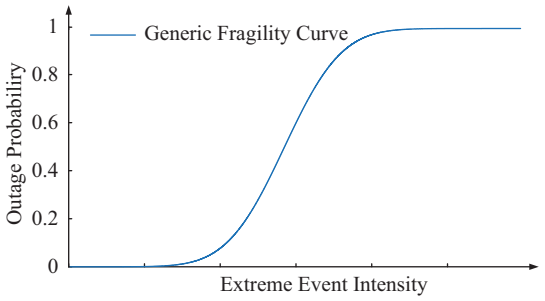

Fig. 2. The generic fragility curve.

fault process. This is because the resilience assessment is executed before extreme events. The number and location of outage lines can generally be fairly predicted during the facility-level resilience assessment [8]–[15]. However, detailed fault process when lines are outage is hard to be well determined before extreme events. For example, will a short circuit fault happen when lines are broken by typhoons? If a short circuit fault will happen, how to predict the detailed fault information, such as fault duration, fault type, and fault location. They are all hard to be effectively predicted before extreme events. The resilience assessment results will be inevitably inaccurate if we consider the fault process, which results in providing wrong decision-making for the resilience control strategy. Therefore, the fault process of accidents caused by extreme events is not considered, and the steady-state system after the accidents is the focus of the system-level resilience assessment of this paper.

The second concern is how to reflect the comprehensive and effectiveness of indices. The security and stability are the permanent and crucial topics for power systems. Especially during extreme events, they are the basic premise for ensuring power supply reliability. Thus, the security and stability indices can quantify the impacts of extreme events on the system resilience in a comprehensive and effective fashion, which are adopted as the resilience assessment indices in this paper.

There are actually many stability and security indices for power systems which can be used to construct the resilience indices, such as the transient stability under large disturbance. However, these indices are not all adopted in this paper. The proposed resilience indices focus more on static stability of system after accidents, i.e., stable operation capability under small disturbance. Since the power system suffers from small disturbances all the time, maintaining its stable operation under small disturbance is the most basic requirement for system survival. If the steady-state system after the accidents cannot withstand small disturbance, this indicates that the system cannot even meet the most basic survival requirement during extreme events and the impacts of extreme events on the resilience is extremely great. Therefore, the static stability, as the most basic operation requirement, is necessary to be used as resilience assessment indices of this paper. As for the transient stability, it is a too rigorous requirement to make the system after the accidents still operate stably under large disturbance. This paper considers that the emergency control of power systems, such as load/generator shedding [27] and DC modulation [28], can help the system after accidents maintain a certain ability to defend against large disturbances. Thus, the transient stability indices are not adopted in this paper.

Except for the above stability indices, security of power systems under extreme events is also a crucial indicator, which needs to be adopted to strengthen the comprehensive of the resilience indices. Some electrical parameters, such as the bus voltage and line current, need to satisfy their security constraints after the accidents. If they violate their security constraints, then the system will still have great operation risk even if the system satisfies the above stability requirements. Furthermore, the static security indicator is also applied in this paper to check the structural strength of system after the accidents. To sum up, the resilience assessment indices constructed in this paper are shown in Fig. 3.

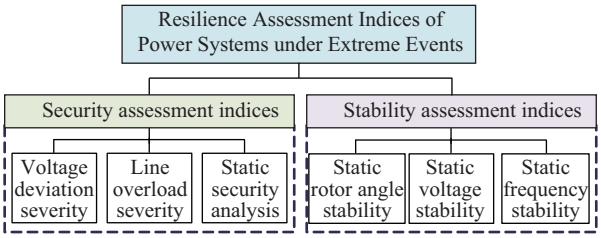

Fig. 3. Resilience assessment indices under extreme events.

The proposed resilience assessment indices contain two essential elements, the security and stability indices. The security indices consist of voltage deviation severity (VDS), line overload severity (LOS), and static security analysis (SSA). The stability indices include three elements, static rotor angle stability (SRAS), static voltage stability (SVS), and static frequency stability (SFS). The proposed resilience indices aims to comprehensively quantify system resilience under extreme events from the aspects of rotor angle, voltage, and frequency etc. The proposed resilience assessment indices are actually the most basic operation requirement for power systems. On the basic of this, the resilience indices can be continually enriched in different scenarios. The specific calculation processes for these resilience assessment indices are shown as follows.

1) Voltage deviation severity

The bus voltage amplitude might violate its limit after contingency lines tripped. Some issues such as voltage instability may be induced if bus voltage violates its constraint. The VDS is shown as follows:

$$\mathrm{Sev}(U) = (U_i - U_{i,\mathrm{nom}})/U_{i,\mathrm{nom}} \tag{1}$$

where U_i denotes the voltage amplitude of bus i; $U_{i,\mathrm{nom}}$ denotes the nominal voltage of bus i.

2) Line overload severity

Multiple lines may be overloaded after contingency lines outage. Line overload is prone to cause cascading outage of power systems. Hence, the situation of line overload needs to be assessed. The essence of line overload can be attributed to line overtemperature [29], and thus it can be quantified from the line temperature. According to IEEE standard [30], the conductor temperature depends on the heat generated by

the conductor itself, the heat absorbed, and dispersed from the outside. Thereby, the transmission line temperature can be depicted as:

$$\frac{\mathrm{d}T_c}{\mathrm{d}t} = \frac{1}{mC_p}(q_j + q_s + q_c + q_r) \tag{2}$$

where T_c is line temperature; m is line quality; q_j is the heat induced by current; q_s is the power of heat absorbed from sun light radiation; q_c is the power of convection heat loss; q_r is the radiation heat emitted from the line. The specific meaning of these parameters are detailed in [30]. Then, the LOS is shown as follows:

$$\mathrm{Sev}(I) = (T_c - T_{c,\max})/T_{c,\max} \tag{3}$$

where $T_{c,\max}$ denotes the highest acceptable temperature of lines under normal operation, which is generally 90°C [31].

3) Static security analysis

The SSA is used to check whether the structural strength of power systems satisfies the requirement of safe operation after the accidents. The method of SSA is the N-1 principle [32]. After the vulnerable lines are outage due to extreme events, the remaining lines will be tripped one by one. If there are no overload lines and buses with voltage violation and the reliable power supply can be ensured after the N-1 check, it indicates that the system can meet the SSA requirement, otherwise the structural strength of the system has been severely damaged by extreme events, which has great operation risk.

4) Static rotor angle stability

The SRAS indicator is used to assess rotor angle stability reserve of power systems after contingency lines outage due to extreme events, shown as follows:

$$K_P = \frac{P_i - P_x}{P_x} \times 100\% \tag{4}$$

where K_P is static rotor angle stability reserve coefficient; P_i is static stable power limit; P_x is power at actual operating conditions.

5) Static voltage stability

The SVS indicator is used to assess voltage stability reserve of the system after the accidents due to extreme events, shown as follows:

$$K_V = \frac{U_x - U_c}{U_x} \times 100\% \tag{5}$$

where K_V is static voltage stability reserve coefficient; U_x is bus voltage amplitude at actual operation conditions; U_c is critical voltage amplitude of bus.

6) Static frequency stability

In addition to the static voltage stability and static rotor angle stability, the static frequency stability is also one of important resilience indices in this paper. Since the proportion of renewable energy is increasing in modern power systems, the system inertia drops dramatically causing frequency stability issues are becoming increasingly prominent. The eigenvalue analysis method and the electromechanical time domain simulation method are two common methods for the static frequency stability analysis [32]. In order to improve the computational efficiency, the eigenvalue analysis method is used to analyze the static frequency stability of the system after the accidents in this paper. If the real parts of all eigenvalues are negative, then the static frequency stability is stable, otherwise it is unstable.

B. Dividing Resilience Levels and Control Strategies

The resilience grading strategy can effectively help operation personnel realize the severity of impacts of extreme events on power systems, which provides decision-making for resilience enhancement strategies. The resilience grading strategy includes resilience assessment indices grading and control strategies grading. First, the proposed resilience assessment indices are graded according to their severity, shown in Table I.

TABLE I
RESILIENCE LEVEL GRADING STRATEGIES

Resilience indices	The level of power system resilience		
	Low	Middle	High
VDS	under -10% or above 30%	[-10%, -5%) or (5%, 30%]	[-5%, 5%]
LOS	above 1.7	(0, 1.7]	under 0
SSA	insecure	–	secure
SRAS	unstable	[0, 10%)	above 10%
SVS	unstable	[0, 8%)	above 8%
SFS	unstable	–	stable

In Table I, each of resilience indicator is categorized into three levels. The higher the resilience level, the smaller the impact of extreme events on the system and the more safely the system can operate. The acceptable voltage deviation is $\pm$ 5% under normal operation [33], and thus the VDS belongs to high resilience level in this case. The voltage should not be lower than 0.9 p.u. after faults, otherwise the system loses voltage stability [34]. Meanwhile, the power frequency overvoltage cannot exceed 1.3 p.u. [35]. Hence, the VDS is at middle resilience level when it belongs to [-10%, -5%) or (5%, 30%], furthermore, the VDS attributes to low resilience level when it is under -10% or over 30%. Since the lines are not overload when the LOS is under 0, the LOS belongs to high resilience level in this case. The lines are overload if their temperature is above 90°C. The lines can operate with 250°C for 5 seconds after faults, i.e., the limit temperature of lines after fault is 250°C [31]. The LOS is lower than 1.7 when the line temperature is under 250°C. Hence, the resilience level is at middle level in this context. The lines cannot operate above 250°C, and thus the resilience level of the LOS is at the low level if it is more than 1.7. The resilience grading method of SSA and SFS is similar. If the system is with static security or static frequency stability after extreme events, then the resilience level is at high level, otherwise it is at low level. The two indices do not have middle resilience level. According to Chinese standard [32], the K_P and K_V should not be less than 10% and 8% after accidents. Therefore, the system resilience is viewed as high level if the K_P and K_V after extreme events are higher than them. The system is stable but its stability reserve is not enough when the K_P is between 0 and 10% and the K_V is between 0 and 8%, thus the resilience level is defined as middle level in this case. The resilience level belongs to low level when the system loses rotor angle stability and voltage stability. The resilience grading strategy in this paper is formulated based on related standards, and

certainly, it can also be adjusted moderately according to real situation.

Thereby, the resilience level of each resilience indicator can be determined by Table I. Any one of the indices violates its operation constraint and the system has great operation risks. For example, if the SRAS reserve is seriously insufficient, the system will have huge operation risks even if the other indicators all meet their operation constraints. Thus, in this paper, a well-known wooden barrel theory in management science [36] is adopted to assess the resilience level of the whole system. The lowest resilience level of all resilience indices is considered as the resilience level of the whole system at this moment. Then, corresponding control strategies for enhancing power system resilience are also divided according to the system resilience levels, shown in Table II.

TABLE II
CONTROL STRATEGY DIVISIONS

Resilience levels	Whether to make a plan	Control type
Low	Yes	Preventive control
Middle	Yes	Post-event control
High	No	No control

In Table II, it does not need a plan and control strategies if the resilience level is at high level since all the resilience indices operate at a normal state. The low resilience level represents that the impact of extreme events on power systems is very great. For instance, the most basic survival requirement of the system, static stability under small disturbance, cannot be ensured. The situation is extremely serious in this case. The post-event control often fails to enhance the resilience well, while preventive control can often show good control effect in this context. Thus, preventive control is used to enhance the low resilience level. The middle resilience level denotes that the impact of extreme events on power systems is general, e.g., the system stability reserve is not sufficient but it can still operate stably. In this case, preventive control and post-event control can generally both improve system resilience well, but post-event control is adopted rather than using the preventive control. The main reason is that preventive control is formulated based on predicted accidents. An inevitable concern is whether the accidents can be predicted accurately. There are certain risks when executing the preventive control. Thus, preventive control should not be executed lightly unless the situation is very serious and post-event control is hard to well defend against extreme event, such as the situation of low resilience level. In other situations, post-event control should be executed as a priority. The specific control principle and available control methods of resilience enhancement strategies for different resilience levels are listed in Table III.

TABLE III
CONTROL PRINCIPLE AND METHOD

Resilience levels	Control principle	Control method
Low	Little load loss	Controlled islanding, etc.
Middle	Without load loss	Generator shedding, etc.
High	–	–

In Table III, the specific control methods are all from the three defensive lines of power systems [22], e.g., post-event control required for middle resilience level is the control strategies in the second and third defensive line, and preventive control required for low resilience level is the preventive control strategies in the first defensive line. When the resilience level is at the low level, since the impact of extreme events on power systems is very great, the load loss induced by resilience enhancement strategies is allowed in this case, but it should be as little as possible. The specific control methods for the low resilience level can be executed from the source, network, and load side of power systems, such as controlled islanding, generator/load shedding. Because the impact of extreme events is general at the middle resilience level, the control principle does not allow load loss in this case. The control methods for the middle resilience level need to be carried out from the source and network side of power systems, which includes generator shedding and DC modulation, etc.

In summary, before extreme events, the system resilience level can be firstly obtained by Table I. The control types are then obtained based on Table II. Finally, the control method with the lowest control cost and the best control effect is executed according to the control principle of Table III to enhance system resilience.

C. A PCI Based Resilience Enhancement Strategy

Most literature is devoted to post-event control, while the preventive control of the first defensive lines is weak in resisting extreme events. Hence, this section will focus on the preventive control required for the low resilience level, and propose a PCI strategy to boost the system resilience. The core of the proposed PCI is to remove contingency lines before extreme events. In other words, the contingency lines will be included in the splitting surface. Then, the system will be split into two islands under the splitting surface before extreme events. When extreme events really come, since the contingency lines have been removed by the controlled islanding, the outage of contingency lines caused by extreme events has no impacts on the system and both islands can operate safely during extreme events. When the impact of extreme events is gone, the two islands are connected and restore to normal operation state before splitting. The proposed PCI aims to ensure secure operation for all islands and power supply for all loads as much as possible under extreme events.

Based on the above idea, determining an appropriate splitting surface that can form self-adequate islands after splitting is another vital issue. Much research has been conducted on solving splitting surface, such as slow coherency method [23], graph theory [24], [25], and heuristic algorithm [26]. In this paper, a mixed integer linear programming (MILP) method based on the authors' prior work [25] is used to determine the splitting surface that can satisfy various splitting constraints.

The controlled islanding can be regarded as a graph partition problem in graph theory. Searching splitting surfaces is to find a set of cut sets satisfying various constraints and divide the graph into several subgraphs. Suppose that there are N lines in the contingency, since the contingency lines need to be included in splitting surface according to the proposed PCI, the buses on both sides of these contingency lines need to belong

to two different islands after splitting, and the constraint can be expressed as:

$$\sum_{k=1}^{N_k} x_{i,k} = 1,\ i \in \Omega_B \tag{6}$$

$$b_l = \begin{cases} 1, & \text{if } x_{i,k} = x_{j,k} \\ 0, & \text{if } x_{i,k} \neq x_{j,k} \end{cases} \tag{7}$$

where $x_{i,k}$ and b_l are binary variables: $x_{i,k} = 1$ denotes that the bus i belongs to island k, otherwise it is 0; $b_l = 1$ represents that the line ij belongs to islands, otherwise the line belongs to the splitting surface; Ω_B is the set of all buses; N_k is the number of islands after splitting. The b_l of (7) can be transformed as:

$$b_l = \sum_{k=1}^{N_k} x_{i,k} \cdot x_{j,k},\ i \in \Omega_B \tag{8}$$

Let $y_k = x_{i,k} \cdot x_{j,k}$. Therefore, the (8) can be transformed as:

$$\begin{cases} b_l = \sum_{k=1}^{N_k} y_k \\ y_k \leq x_{i,k}, y_k \leq x_{j,k} \\ y_k \geq x_{i,k} + x_{j,k} - 1 \\ y_k \in (0,1) \end{cases} \tag{9}$$

The contingency lines can be included in splitting surfaces from the constraints (6) to (9). Other constraints of controlled islanding, such as the connectivity constraint of islands after splitting, the voltage amplitude constraint, and the power balance constraint, are detailed in [25]. The objective function for determining splitting surfaces is usually minimizing the load shedding and minimizing the power flow disruption in current research. Minimizing the load shedding is as the objective function of the proposed PCI in this paper since the preventive control strategy should cause as little load loss as possible, which is shown as:

$$\min \sum_{i=1}^{N_b} (P_{Di}^{\max} - P_{Di}),\ i \in \Omega_B \tag{10}$$

where N_b is the number of buses; $P_{Di}^{\max}$ is the load active power of bus i before splitting; P_{Di} is the load active power of bus i after splitting. Then, the splitting surface that satisfies the objective function (10) and various splitting constraints can be determined based on the MILP method [25].

IV. Simulation Tests

In this section, the typhoon disaster of extreme events is taken as an example, and a real power system located in the east coast of China is used to test the proposed method. In order to give a deeper insight of the proposed method, two real typhoons that ever hit the system in 2019 and 2020, named Lekima and Hagupit, are respectively applied in the test system to verify the proposed method. The test system and the trajectories of the two typhoons are shown in Fig. 4.

The system contains 108 buses, where the active powers of all generators and loads are 4125 MW and 4080 MW respectively in the system. The red dotted curve in Fig. 4 denotes the moving trajectory of the Lekima, and that of the Hagupit is the blue curve. The latitude and longitude of the two

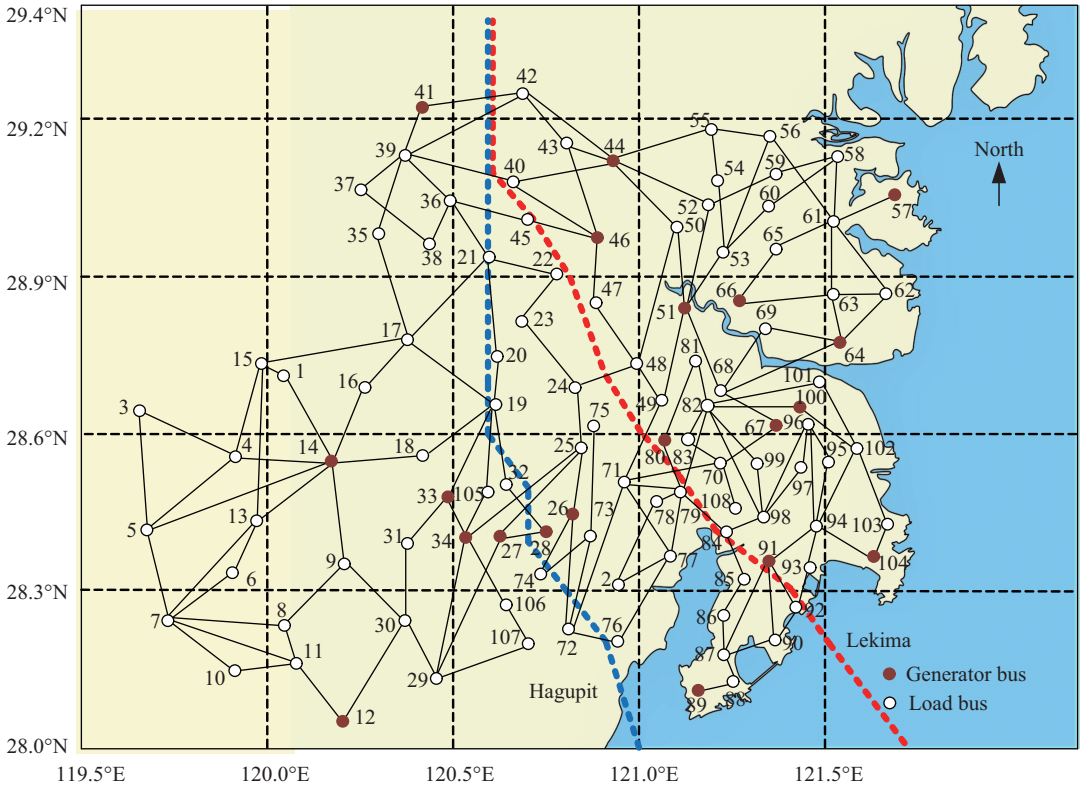

Fig. 4. Test system and typhoon trajectories.

typhoons' center at different moments are predicted by [37]. Meanwhile, two severe rainstorms were originated by both typhoons, and the 24-hour rainfall caused by them in the region were both 300–500 mm. Next, the two typhoons are imposed on the system respectively to test the proposed method.

A. Simulation for Resilience Assessment Methods

The facility-level resilience assessment is conducted firstly. Transmission lines and towers are generally more likely to be subject to damages of typhoons [10], and thus the lines and towers are the focus of the facility-level resilience assessment in this paper. The fragility surfaces of lines and towers of the system under typhoons and rainstorms are shown in Fig. 5.

The fragility surfaces of Fig. 5 were generated from the authors' previous work [8], where the material parameters of lines and towers are the most common type in the system. The fragility surfaces reflect the failure probability of transmission lines and towers under different typhoon wind speed and rainfall intensity. The simulation step is an hour since the typhoon forecast information is updated every hour. We only use the prediction information of current moment to predict the outage probability at the next moment. This can ensure the accuracy of prediction. Thereby, the outage probabilities of all lines due to each of the two typhoons at different moments can be determined respectively by the method of [8], where those of partial lines are shown in Fig. 6.

It can be seen from Fig. 6 that the outage probabilities decrease over time, as the typhoon wind speed drastically drops after landing. The long-term operation experience in the system indicates that the outage probability threshold of lines is about 0.1 due to typhoons. Therefore, the lines with outage probabilities higher than the outage threshold are viewed as contingency lines at each moment. Thereby, the contingency lines caused by the Lekima are L87-91 at the moment 1, L70-67 and L82-79 at the moment 2, and L68-64 and L71-72 at the moment 3. There are no lines with outage probability higher than the threshold after the moment 3. Meanwhile, the contingency lines due to the Hagupit are also available, i.e., L91-87 and L77-76 at the moment 1, as well as the L29-27 and L25-34 at the moment 2. The system has no contingency lines after the moment 2. Then, the system resilience of each moment after each of the two typhoons can be obtained based on the proposed resilience assessment indices, which is shown in Tables IV and V respectively.

TABLE IV
RESILIENCE ASSESSMENT RESULTS UNDER THE LEKIMA

Resilience indices	Moment 1	Moment 2	Moment 3
VDS	−4.81%	−6.16%	–
LOS	−0.39	−0.31	–
SSA	secure	secure	insecure
SRAS	10.36%	8.42%	unstable
SVS	8.7%	5.69%	unstable
SFS	stable	stable	unstable

TABLE V
RESILIENCE ASSESSMENT RESULTS UNDER THE HAGUPIT

Resilience indices	Moment 1	Moment 2
VDS	−6.53%	–
LOS	−0.28	–
SSA	secure	insecure
SRAS	8.71%	unstable
SVS	3.94%	unstable
SFS	stable	unstable

In Tables IV and V, the VDS and the LOS are the most serious value of all buses and lines at different moments. The SRAS reserve coefficient and SVS reserve coefficient are the smallest value of the all buses. In Table IV, since the resilience indices are with normal operation at moment 1, the resilience level is at high level at this moment and no resilience control strategies need to be carried out. At the moment 2, other resilience indices are at high resilience level, while the SRAS, VDS, and SVS violate their operation constraints. According to the proposed resilience level and control strategies grading strategies, the resilience level of the whole system belongs to middle level in this case, and post-event control should be executed to enhance the resilience. At the moment 3, the system stability has been damaged and all resilience indices operate at low resilience level, denoting that

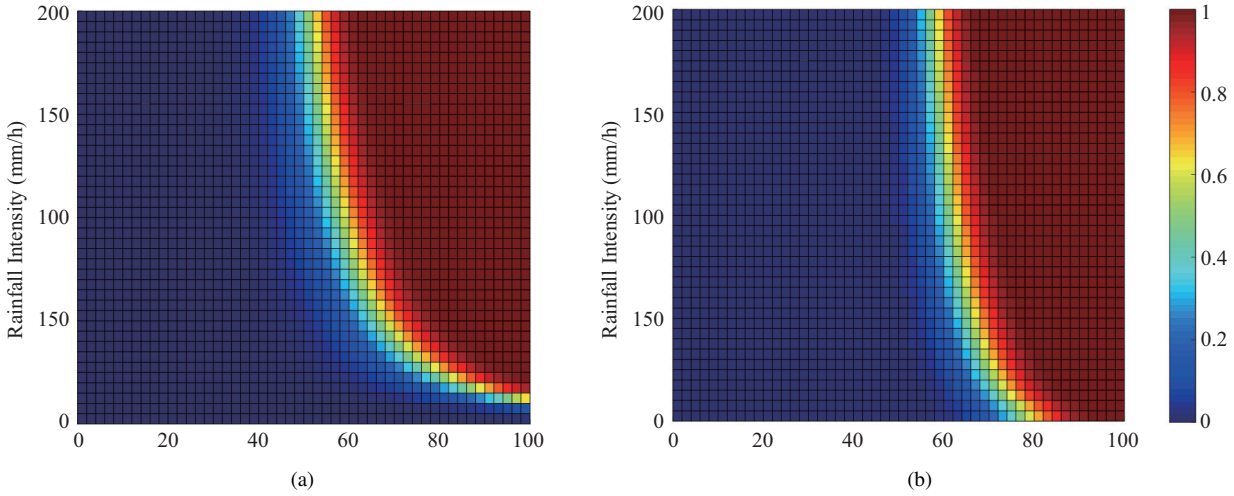

Fig. 5. Failure probability of lines and towers. (a) Outage probability of line spans. (b) Outage probability of towers.

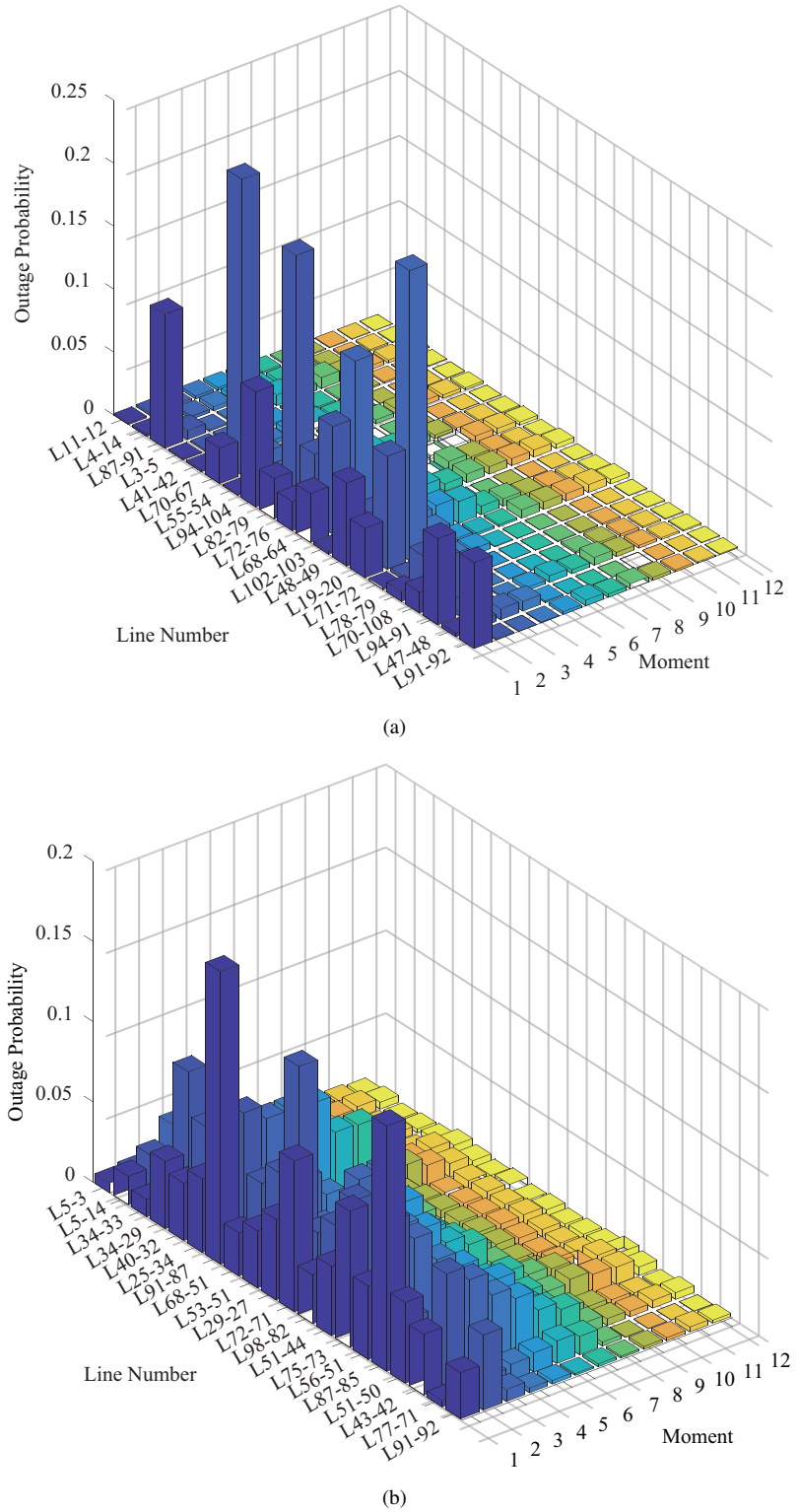

Fig. 6. Outage probability of partial lines due to each of the two typhoons. (a) Outage probability due to Lekima. (b) Outage probability due to Hagupit.

the system has been collapsed and resilience level of the whole system is at low level and the preventive control is urgent to be implemented. Similarly, in Table V, the resilience level of the whole system respectively belongs to middle level and low level at moment 1 and moment 2. The post-event control and the preventive control need to be enforced respectively to enhance the system resilience under different moments.

After resilience assessment using the proposed resilience indices, the resilience level of each resilience indicator and the resilience level of the whole system can be determined based on the proposed resilience grading strategy. Then, corresponding resilience control strategies and their guidelines can be formulated based on the resilience grading results, which helps power systems resist extreme events. From Tables IV

and V, the proposed resilience assessment indices could assess the system resilience from the security and stability of the whole system, which is more comprehensive and effective than current resilience indicators.

B. Simulation for Resilience Enhancement Strategies

This section will focus on testing the control effect of the proposed PCI. Thus, it is assumed that there is no post-event control in the system. The proposed PCI is used to enhance the system resilience against the Lekima firstly. The system resilience is at low level due to the Lekima at the moment 3, and thus the proposed PCI should be carried out at the moment 2 to enhance the resilience of the moment 3. According to the core idea of the proposed PCI, the splitting surface should include the contingency lines L68-64 and L71-72 at the moment 3 to remove their impacts in advance. Moreover, to form self-adequate islands after splitting, several security constraints listed in the Section III.C and the objective function of minimizing the load shedding need to be satisfied. Then, the splitting surface can be determined as L64-68, L68-69, L51-53, L51-52, L51-50, L49-48, L71-72 and L72-76 using the MILP method of [25], shown in Fig. 7.

In Fig. 7, the splitting surface includes the contingency lines L68-64 and L71-72 of the moment 3, and two islands, island A near the west and island B near the east, are formed after splitting. Since the power between generators and loads are generally unbalanced for each island after splitting, generator/load shedding need to be executed to balance the power. The 288 MW generator shedding and 295 MW load shedding need to be executed to balance the power of the two islands using the method of [25]. Thereby, the control cost of the proposed PCI is the load loss of 295 MW in this case. Then, the resilience assessment for the island A and island B using the proposed resilience indices is carried out to verify the control effect of the PCI, shown in Table VI.

TABLE VI
RESILIENCE ASSESSMENT RESULTS FOR ISLAND A AND B

Resilience Indices	Island A	Island B
VDS	−4.19%	4.45%
LOS	−0.32	−0.24
SSA	secure	secure
SRAS	12.15%	12.92%
SVS	11.10%	9.86%
SFS	stable	stable

In Table VI, all the resilience indices of the two islands are at high resilience level, representing that the whole system resilience is at high level after the PCI. Since the contingency lines have been removed by the PCI in advance, the system can operate at this high resilience level when the Lekima really comes. Thus, the proposed PCI can effectively enhance the system resilience against the Lekima.

To further verify the effectiveness of the proposed PCI, it is further used to enhance the system resilience against the Hagupit. Since the resilience level of the whole system caused by the Hagupit is at low level at the moment 2, the proposed PCI needs to be carried out at the moment 1 to enhance the system resilience at the moment 2. The contingency lines caused by the Hagupit are the L29-27 and L25-34 at the moment 2, and they need to be removed in advance by the

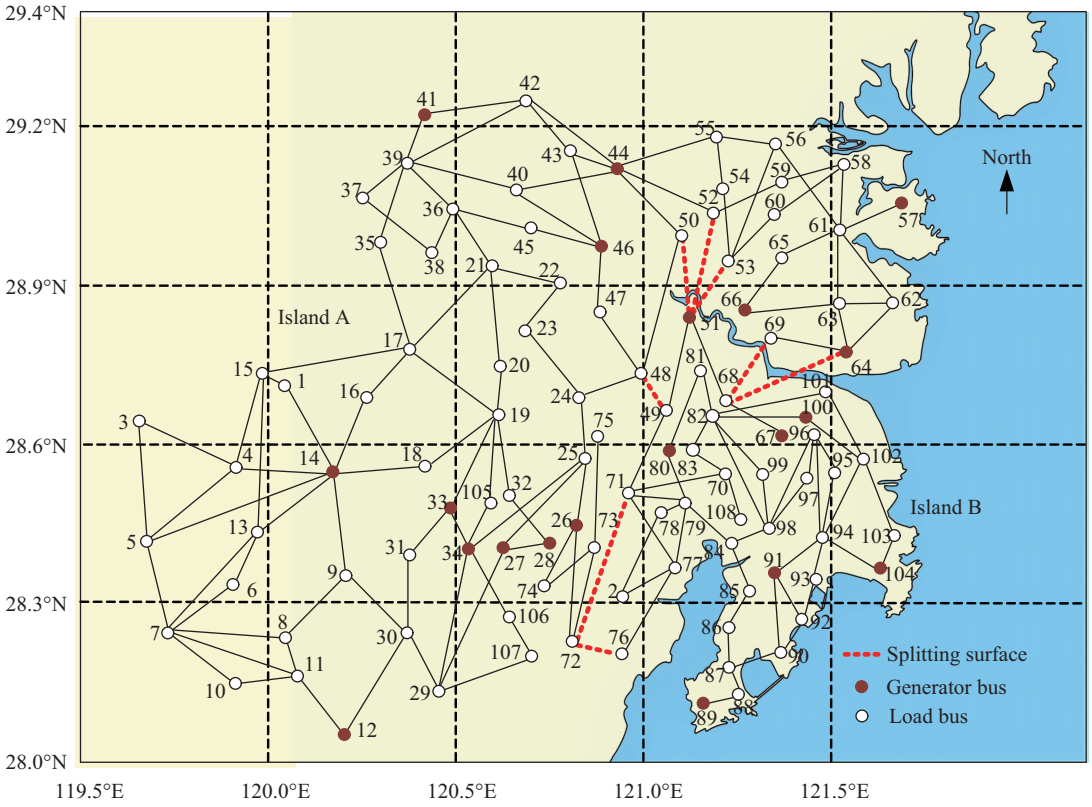

Fig. 7. Splitting surface based on the proposed PCI under the Lekima.

proposed PCI. Herewith, the splitting surface that contains the contingency and satisfies various splitting constraints can be obtained using the MILP [25], i.e., L15-17, L16-17, L18-19, L33-19, L34-105, L34-25, and L27-29, shown in Fig. 8.

It can be seen from Fig. 8 that two islands, island C and island D, are formed after the proposed PCI, and the contingency lines have been removed. A total of 340 MW load shedding needs to be executed after splitting to balance the power, and thus the control cost caused by the PCI in this case is 340 MW load loss. The resilience of the island C and D is assessed by the proposed resilience indices to verify the control effect of the PCI, shown in Table VII.

TABLE VII
RESILIENCE ASSESSMENT RESULTS FOR ISLAND C AND D

Resilience Indices	Island C	Island D
VDS	4.92%	4.91%
LOS	−0.24	−0.29
SSA	secure	secure
SRAS	14.81%	13.90%
SVS	10.13%	9.63%
SFS	stable	stable

In Table VII, the resilience levels of all resilience indices for the two islands after the proposed PCI are at high level, which indicates that the whole system is at high resilience level when the Hagupit really comes. Therefore, the proposed PCI can help the system defend against the two typhoons with good control effect and low control cost. Moreover, the first defensive line of power systems can actually play a vital role in defending against extreme events and enhancing power system resilience, which is well worth being reinforced.

C. Comparison Between the Preventive Control and the Post-event Control

In order to verify the advantage of the preventive control in boosting the low resilience level, the post-event control is tested to compare with the preventive control in this section. The controlled islanding in post-event control, i.e., the second defensive line of power systems, is used to resist the two typhoons in this section. For ease of illustration, the controlled islanding in post-event control is called as traditional controlled islanding (TCI) in the following. Since the proposed PCI and the TCI are both involved in the controlled islanding, the preventive control and the post-event control can be compared by them in a more reasonable fashion. Due to the limitation of space, the comparison is only conducted by Lekima. The TCI is to separate generators losing coherency into different islands to prevent transient instability of the system after accidents. A plan needs to be formulated for the TCI before accidents, and then the TCI should be executed after accidents. The coherency of all generators after the contingency tripped at the moment 3 is shown in Table VIII through the time domain simulation.

The coherency of all generators will be divided into four

TABLE VIII
THE COHERENCY OF GENERATORS AFTER THE LEKIMA

Coherency group	Generator buses
1	12
2	28
3	67
4	Other generators

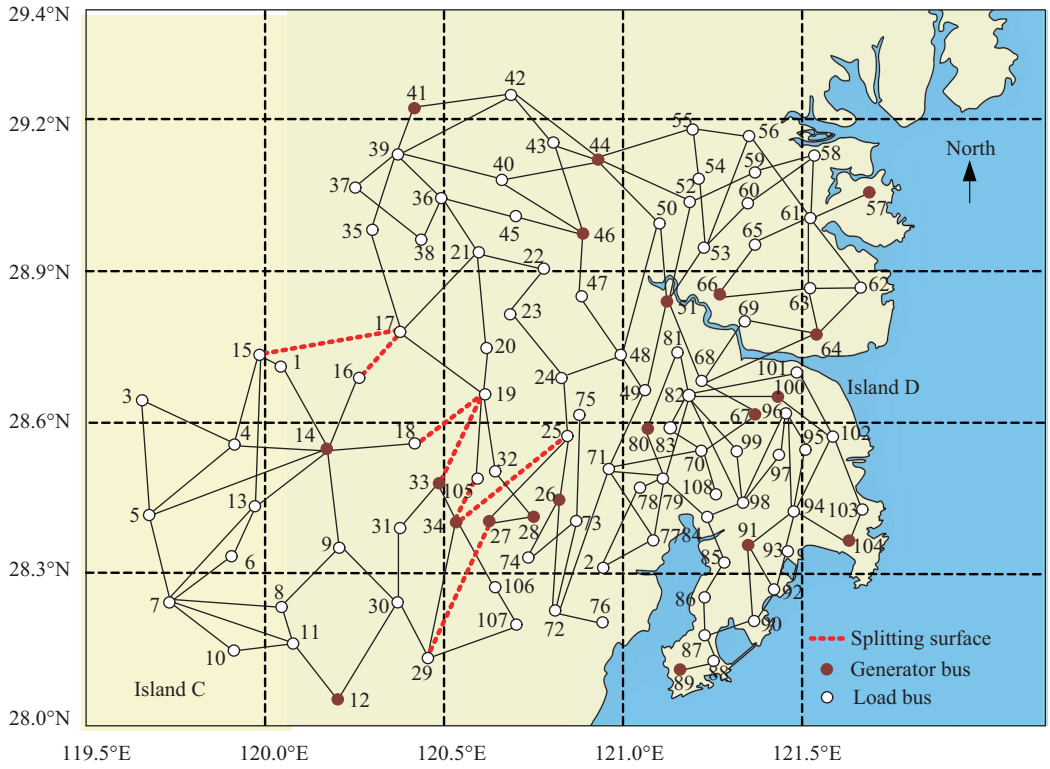

Fig. 8. Splitting surface based on the proposed PCI under the Hagupit.

groups after the contingency lines tripped from Table VIII. Therefore, the number of islands after the TCI is four, and these generators losing coherency should be respectively separated into four islands. To better compare the control effect, the objective function and security constraints of the TCI are the same as the proposed PCI when determining the splitting surface. Then, the splitting surface obtained by the TCI can be determined as L5-7, L7-13, L6-13, L8-9, L12-30, L32-28, L27-28, and L68-67 using the MILP [25], shown in Fig. 9.

The system is separated into four islands from Fig. 9, and those generators losing coherency are separated respectively. It can be observed that the generator 67 and 28 are split from the whole system, forming two islands, each only with one generator bus, which causes the whole system to lose two generators. The island E and island F are the two islands with generators and loads after splitting. A total of 687 MW load shedding needs to be executed after the TCI to balance the power of each island, and thus its control cost is 687 MW load loss. The control effect of the TCI is assessed by the proposed resilience assessment indices, shown in Table IX.

TABLE IX
RESILIENCE ASSESSMENT RESULTS FOR ISLAND E AND F

Resilience Indices	Island E	Island F
VDS	−5.57%	4.53%
LOS	−0.19	−0.36
SSA	insecure	secure
SRAS	9.16%	10.25%
SVS	5.53%	9.87%
SFS	stable	stable

In Table IX, all the resilience indices of island F are at high resilience level, indicating that the resilience of the island F is at high level. However, the condition is not optimistic for the island E. The VDS, SRAS, and SVS violates their operation constraints, belonging to middle resilience level. The SSA of island E is insecure since the island has only one generator bus 12 and the generator has only one transmission line L11-12 to other loads. During the SSA, all the loads of island E will be lost if the L11-12 is tripped, which indicates that the structural strength of island E is damaged severely after the TCI, and the resilience level of island E is at low level.

The comparison of the proposed PCI and the TCI under the Lekima in control effect and control cost is detailed in Table X. In Table X, the control effect is represented by the resilience level after the two control strategies. Obviously, the higher resilience level of each island after the two control strategies, the better the control effect. The control cost is quantified by the system load loss after the two control strategies. The control cost is satisfying when the load loss is little.

TABLE X
COMPARISON BETWEEN THE PROPOSED PCI AND THE TCI

The proposed PCI		The TCI	
control effect	control cost	control effect	control cost
high level	295 MW	low level	687 MW

From Table X, the islands after the proposed PCI are all at high resilience level, while there are islands with low resilience level after the TCI. This indicates that the proposed PCI has better control effect than that of the TCI. Since the number

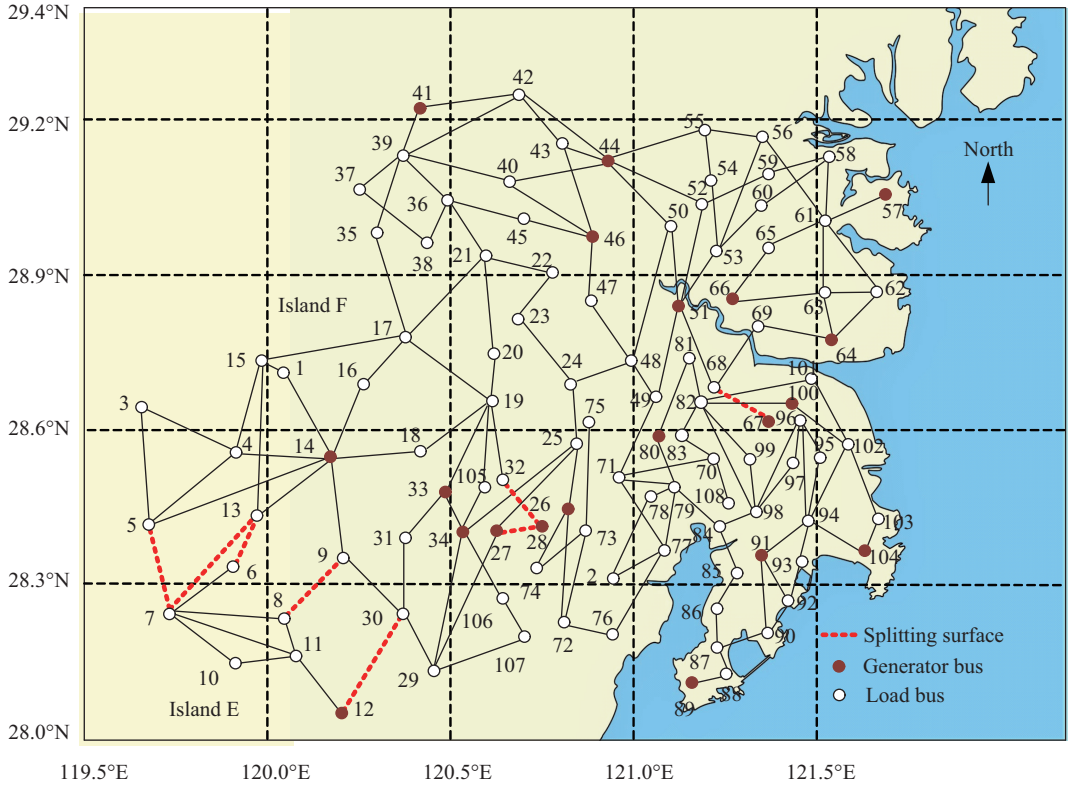

Fig. 9. Splitting surface obtained by the TCI under the Lekima.

of islands after the TCI is large and some generators are lost, the number of load shedding after the TCI is more than that of the proposed PCI, and then the control cost of the TCI is higher than that of the proposed PCI. Hence, when the impact of extreme events is very great causing the system resilience level is quite low, the preventive control can show better control effect and lower control cost than that of the post-event control in boosting system resilience. The post-event control is hard to enhance the system resilience well in this case, which needs additional control measures to remedy. However, the preventive control can display excellent control effect, and thus it Is crucial to strengthen the first defensive line of power systems to defend against extreme events.

D. Comparison of Different PCI Strategies

To give a further insight to the proposed method, in this section, the PCI of [21] is used to compare with the proposed PCI of this paper. The core idea of [21] is to isolate all contingency lines with higher outage probability into an island before extreme events to prevent the spread of the impacts due to these contingency lines tripped. The load loss is the resilience assessment indicator in [21], which provides decision-making for the PCI. To better comparison, in this paper, the proposed resilience assessment indices are used to provide decision-making for the PCI of [21]. Due to the limitation of space, the comparison is only conducted by Lekima, where the PCI of [21] is executed at the moment 2 to boost the system resilience at the moment 3. Without losing generality, the MILP of [25] is also applied to determine the splitting surface, and the constraint and objective function are the same as the PCI of this paper. Thus, the splitting surface based on the idea of PCI [21] can be determined as L63-64, L62-64, L51-53, L51-52, L51-50, L48-49 and L25-26 using the MILP [25], shown in Fig. 10.

After the PCI of [21], two islands, island G near the west and island H near the east, are formed, where the island G does not contain contingency lines L68-64 and L71-72, and contingency lines are all isolated into the island H. The 315 MW load shedding needs to be executed after the PCI of [25] to balance the power of both islands. It can be seen that the scale of island H is large since the contingency lines are with far electrical distance. Then, the resilience of the two islands after the contingency lines tripped due to the Lekima is assessed, shown in Table XI.

TABLE XI
RESILIENCE ASSESSMENT RESULTS FOR ISLAND G AND H

Resilience Indices	Island G	Island H
VDS	−4.90%	−7.34%
LOS	−0.24	−0.15
SSA	secure	secure
SRAS	12.18%	5.32%
SVS	10.65%	2.05%
SFS	stable	stable

In Table XI, the island G can operate at the high resilience level when the Lekima comes since there are no contingency lines in the island. The island H includes two contingency lines after the PCI of [21], causing its stability reserve is not

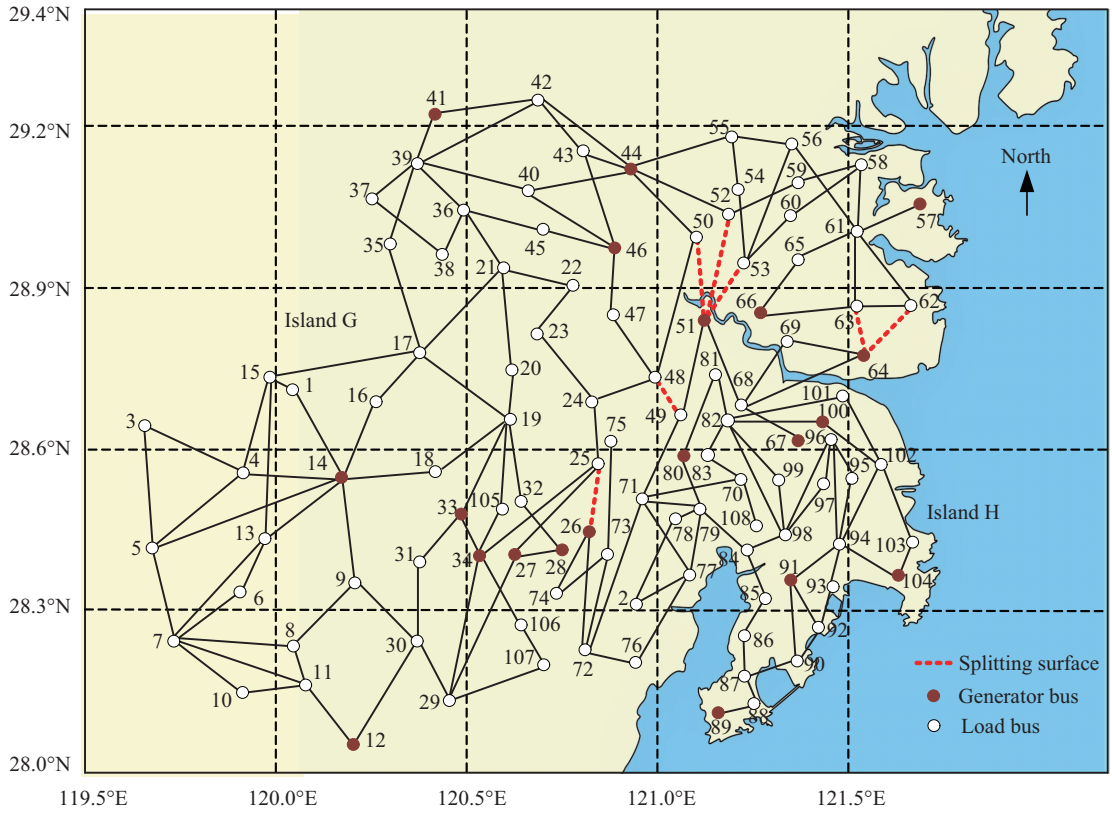

Fig. 10. Splitting surface based on the PCI of [21] under the Lekima.

sufficient after the contingency lines tripped, and the resilience of the island H belongs to middle level. Thus, there is an island with middle resilience level when the PCI of [21] is used to resist the Lekima. The control effect and control cost induced by the proposed PCI and the PCI of [21] are listed in Table XII.

TABLE XII
COMPARISON BETWEEN THE PROPOSED PCI AND THE PCI OF [21]

The proposed PCI		The PCI of [21]	
control effect	control cost	control effect	control cost
high level	295 MW	middle level	315 MW

In Table XII, the control costs of the two PCI strategies under the two typhoons are both induced by the load shedding after splitting, which has not many gaps between them. The islands after the proposed PCI are all at high resilience level since the contingency lines are removed in advance. However, because there are contingency lines in an island after the PCI of [21], the resilience of one of the islands with contingency lines must be influenced. For instance, after enforcing the PCI of [21], there is an island H with middle resilience level after the Lekima. This indicates that the proposed PCI has better control effect than that of the PCI of [21] in defending against the Lekima. However, this cannot demonstrate that the control effect of the proposed PCI is better than that of the PCI of [21] in all cases. Strictly speaking, the comparison of the two PCI strategies is easily affected by various factors such as the typhoon trajectory and system structure. Hence, the two PCI strategies could show respective advantages in different scenarios. The proposed PCI and the PCI of [21] could be viewed as complementary. The organic combination of the two PCI strategies can provide more secure operation for power systems under extreme events, and this will be studied in our future work.

V. CONCLUSION

This paper has presented a unified framework for preventive control of power systems to enhance the system resilience against extreme events. The framework includes three components: resilience assessment, resilience grading, and resilience enhancement. The proposed resilience assessment indices can reflect system resilience from the safe and stable operation of the whole system, which is more comprehensive and effective than current resilience assessment indices. The proposed PCI can ensure security operation for all islands after splitting and provides the reliable power supply for all loads as much as possible, which drastically enhances power system resilience. The preventive control of power systems can actually show preferable control effect, which well deserves to be reinforced to resist extreme events.

Similar to the TCI, the proposed PCI is also a dispatch strategy, which contributes the operation personnel of power systems to make decision-making under extreme events. However, in contrast to the TCI, the dispatch strategy of PCI is formulated and executed before extreme events, and it is updated every once in a while, which depends on the prediction frequency of extreme events. For instance, in this paper, since the typhoon prediction information is updated every hour, the dispatch strategy of PCI is also updated every hour. Before extreme events, the facility-level resilience is assessed according to the prediction information. Once some facilities are predicted to be damaged, then the proposed method, i.e., system-level resilience assessment, resilience grading, and enhancement strategies, will be immediately carried out. The proposed method will be implemented in the entire period of extreme events until their impacts disappear.

In summary, when the proposed method in this paper is used in practice, it is mainly aimed at the transmission network of 110 kV and above. The network size is one city or several surrounding cities, depending on the impact ranges of extreme events. The costs caused by the proposed method are quantified by load loss in this paper. The smaller the load loss induced by the PCI, the lower the cost. Some other costs, such as the economic costs after the PCI, are also well worth being considered, which will be investigated in our future work. Moreover, the proposed method is more suitable to cope with extreme events which can be predicted, such as typhoons, rainstorms, and snowstorms. In practice, some extreme events, such as artificial attack, are often hard to be predicted before happening since they have very intense human subjectivity. If the proposed method is applied to defend against these extreme events, a potential method is to seek weak points of power systems in advance, and then formulates the PCI strategy. This valuable work will be studied in the future work.

REFERENCES

[1] H. Hou, S. W. Yu, X. Q. Li, H. B. Wang, Y. Huang, and X. X. Wu, "Early warning for transmission line damage under typhoon disaster based on random wind field probability weighting," *Automation of Electric Power Systems*, vol. 45, no. 7, pp. 140–147, Apr. 2021.

[2] G. L. Zhang, H. W. Zhong, Z. F. Tan, T. Cheng, Q. Xia, and C. Q. Kang, "Texas electric power crisis of 2021 warns of a new blackout mechanism," *CSEE Journal of Power and Energy Systems*, vol. 8, no. 1, pp. 1–9, Jan. 2022.

[3] C. S. Holling, "Resilience and stability of ecological systems," *Annual Review of Ecology and Systematics*, vol. 4, pp. 1–23, 1973.

[4] Y. Yuan, H. Zhang, H. Z. Cheng, Z. Wang, and J. P. Zhang, "Resilience-oriented transmission expansion planning with optimal transmission switching under typhoon weather," *CSEE Journal of Power and Energy Systems*, to be published, 2021, doi: 10.17775/CSEEJPES.2021.07840.

[5] W. Tang, Z. Q. Wang, L. Zhang, B. Zhang, J. Liang, K. Y. Liu, and W. X. Sheng, "Optimal allocation strategy of electric EPSVs and hydrogen fuel cell EPSVs balancing resilience and economics," *CSEE Journal of Power and Energy Systems*, to be published, 2021, doi: 10.17775/CSEEJPES.2021.05430.

[6] Y. Z. Wang, C. Chen, J. H. Wang, and R. Baldick, "Research on resilience of power systems under natural disasters—a review," *IEEE Transactions on Power Systems*, vol. 31, no. 2, pp. 1604–1613, Mar. 2016.

[7] Z. H. Bie, Y. L. Lin, G. F. Li, and F. R. Li, "Battling the extreme: a study on the power system resilience," *Proceedings of the IEEE*, vol. 105, no. 7, pp. 1253–1266, Jul. 2017.

[8] Z. P. Wang, Y. W. Xiang, and T. Wang, "Assessment method of tower falling and line disconnection accidents for 110 kV line in typhoon and torrential rain disaster," *Automation of Electric Power Systems*, vol. 46, no. 3, pp. 59–66, Feb. 2022.

[9] S. Espinoza, A. Poulos, H. Rudnick, J. C. de la llera, M. Panteli, and P. Mancarella, "Risk and resilience assessment with component criticality ranking of electric power systems subject to earthquakes," *IEEE Systems Journal*, vol. 14, no. 2, pp. 2837–2848, Jun. 2020.

[10] X. N. Liu, K. Hou, H. J. Jia, J. B. Zhao, L. Mili, X. L. Jin, and D. Wang, "A planning-oriented resilience assessment framework for transmission systems under typhoon disasters," *IEEE Transactions on Smart Grid*, vol. 11, no. 6, pp. 5431–5441, Nov. 2020.

[11] M. Panteli, C. Pickering, S. Wilkinson, R. Dawson, and P. Mancarella, "Power system resilience to extreme weather: fragility modeling, probabilistic impact assessment, and adaptation measures," *IEEE Transactions on Power Systems*, vol. 32, no. 5, pp. 3747–3757, Sep. 2017.
[12] M. Panteli and P. Mancarella, "Modeling and evaluating the resilience of critical electrical power infrastructure to extreme weather events," *IEEE Systems Journal*, vol. 11, no. 3, pp. 1733–1742, Sep. 2017.
[13] M. Panteli, P. Mancarella, D. N. Trakas, E. Kyriakides, and N. D. Hatziargyriou, "Metrics and quantification of operational and infrastructure resilience in power systems," *IEEE Transactions on Power Systems*, vol. 32, no. 6, pp. 4732–4742, Nov. 2017.
[14] M. Panteli, D. N. Trakas, P. Mancarella, and N. D. Hatziargyriou, "Power systems resilience assessment: hardening and smart operational enhancement strategies," *Proceedings of the IEEE*, vol. 105, no. 7, pp. 1202–1213, Jul. 2017.
[15] P. Akaber, B. Moussa, M. Debbabi, and C. Assi, "Automated post-failure service restoration in smart grid through network reconfiguration in the presence of energy storage systems," *IEEE Systems Journal*, vol. 13, no. 3, pp. 3358–3367, Sep. 2019.
[16] S. H. Yao, P. Wang, X. C. Liu, H. J. Zhang, and T. Y. Zhao, "Rolling optimization of mobile energy storage fleets for resilient service restoration," *IEEE Transactions on Smart Grid*, vol. 11, no. 2, pp. 1030–1043, Mar. 2020.
[17] Y. Xu, C. C. Liu, K. P. Schneider, F. K. Tuffner, and D. T. Ton, "Microgrids for service restoration to critical load in a resilient distribution system," *IEEE Transactions on Smart Grid*, vol. 9, no. 1, pp. 426–437, Jan. 2018.
[18] Z. W. Wang, C. Shen, Y. Xu, F. Liu, X. Y. Wu, and C. C. Liu, "Risk-limiting load restoration for resilience enhancement with intermittent energy resources," *IEEE Transactions on Smart Grid*, vol. 10, no. 3, pp. 2507–2522, May 2019.
[19] Z. Y. Wang, B. K. Chen, J. H. Wang, and C. Chen, "Networked microgrids for self-healing power systems," *IEEE Transactions on Smart Grid*, vol. 7, no. 1, pp. 310–319, Jan. 2016.
[20] G. Huang, J. H. Wang, C. Chen, J. J. Qi, and C. X. Guo, "Integration of preventive and emergency responses for power grid resilience enhancement," *IEEE Transactions on Power Systems*, vol. 32, no. 6, pp. 4451–4463, Nov. 2017.
[21] M. Panteli, D. N. Trakas, P. Mancarella, and N. D. Hatziargyriou, "Boosting the power grid resilience to extreme weather events using defensive islanding," *IEEE Transactions on Smart Grid*, vol. 7, no. 6, pp. 2913–2922, Nov. 2016.
[22] *Technical Guide for Electric Power System Security and Stability Control*, GB/T 26399-2011, 2011.
[23] G. Y. Xu and V. Vittal, "Slow coherency based cutset determination algorithm for large power systems," *IEEE Transactions on Power Systems*, vol. 25, no. 2, pp. 877–884, May 2010.
[24] L. Ding, F. M. Gonzalez-Longatt, P. Wall, and V. Terzija, "Two-step spectral clustering controlled islanding algorithm," *IEEE Transactions on Power Systems*, vol. 28, no. 1, pp. 75–84, Feb. 2013.
[25] Y. W. Xiang, T. Wang, and Z. P. Wang, "Protection information based transient stability margin assessment of splitting islands," *International Journal of Electrical Power & Energy Systems*, vol. 130, pp. 107007, Sep. 2021.
[26] Y. J. Wu, Y. Tang, B. Han, and M. Ni, "A topology analysis and genetic algorithm combined approach for power network intentional islanding," *International Journal of Electrical Power & Energy Systems*, vol. 71, pp. 174–183, 2015.
[27] S. X. Zhu, T. Wang, and Z. P. Wang, "Bi-level optimised emergency load/generator shedding strategy for AC/DC hybrid system following DC blocking," *IET Generation, Transmission & Distribution*, vol. 14, no. 8, pp. 1491–1499, Apr. 2020.
[28] T. Wang, C. C. Li, D. K. Mi, Z. P. Wang, and Y. W. Xiang, "Coordinated modulation strategy considering multi-HVDC emergency for enhancing transient stability of hybrid AC/DC power systems," *CSEE Journal of Power and Energy Systems*, vol. 6, no. 4, pp. 806–815, Dec. 2020.
[29] J. Hu, X. F. Xiong, and J. Wang, "Current tolerance capability calculation model of transmission lines and its application in overload protection," *Electric Power Components and Systems*, vol. 46, no. 14–15, pp. 1509–1521, Jul. 2018.
[30] *IEEE Standard for Calculating the Current-Temperature Relationship of Bare Overhead Conductors*, IEEE Standard 738-2012, 2013.
[31] *Power Cables with Extruded Insulation and Their Accessories for Rated Voltages Above 30 kV (U_m = 36 kV) up to 150 kV (U_m = 170 kV)-Test Methods and Requirements*, IEC International Standard 60840, 2020.
[32] *Code on Security and Stability for Power System*, GB 38755-2019, 2019.
[33] *Power Quality-Deviation of Supply Voltage*, GB/T 12325-2008, 2009.
[34] *Guide on Security and Stability Analysis for CSG*, Q/CSG 11004-2009, 2009.
[35] *Power Quality-Temporary and Transient Overvoltages*, GB/T 18481-2001, 2004.
[36] G. E. Rejda, *Risk Management and Insurance*, 5th ed., Harper Collins College Press, 1995.
[37] National Meteorological Centre. [Online]. Available: http://www.nmc.cn

Yuwei Xiang received the B.S. degree from Lanzhou University of Technology, Lanzhou, China, in 2018. He is currently working toward the Ph.D. degree in Electrical Engineering at North China Electric Power University, Beijing, China. His main research interests include power system risk assessment, and power system stability analysis and control.

Tong Wang received B.S. and Ph.D. degrees from North China Electric Power University, China, in 2007 and 2013, respectively. She was a Visiting Researcher Scholar from 2011 to 2012 in the Bradley Department of Electrical and Computer Engineering, Virginia Polytechnic Institute and State University, USA. She is currently an Associate Professor in the School of Electrical and Electronic Engineering, North China Electric Power University, China. Her interests mainly include stability analysis and emergency control for power system.

Zengping Wang received B.S. and M.S. degrees in Electric Engineering from North China Electric Power University, China, in 1985 and 1988, respectively. He received the Ph.D. degree from the Harbin Institute of Technology, China, in 1997. He is currently the Professor and Vice President of North China Electric Power University. His special fields of interest include relay protection, fault analysis and system security protection.